DOI: 10.1007/s12541-012-0283-0

Computational Analyses of Pinching Dynamics of a Finger Exoskeleton Composed of IPMC Actuators

Soo Jin Lee[1], Yoon Jeong Kim[1], Gwang Hun Jeong[1], Bye Ri Yoon[2], Jae Young Jho[2], Dong Min Kim[3], and Kyehan Rhee[1,#]

1 Department of Mechanical Engineering, College of Engineering, Myongji University, Yongin, South Korea, 449-728
2 Department of Chemical and Biological Engineering, College of Engineering, Seoul National University, Seoul, South Korea, 151-742
3 Department of Electrical Engineering, College of Engineering, Hongik University, Jochiwon, South Korea, 339-701
Corresponding Author / E-mail: khanrhee@mju.ac.kr, TEL: +82-31-330-6426, FAX: +82-31-321-4959

KEYWORDS: Finger exoskeleton, Ionic polymer metal composite, Dynamics simulation, Electromechanical characteristics, Biomechanics

There is an increased demand for hand exoskeletons that are light weight, low profile, and flexible, and that consume less power. In order to replace the rigid actuators such as motors and pneumatic cylinders, an ionic polymer metal composite (IPMC) actuator may be a good candidate. Because of the limited forces generated by IPMC actuators, prediction of the IPMC actuation force for the required fingertip force is important in designing and improving the performance of a finger exoskeleton. Anthropomorphic data on index fingers and the stiffness of a finger joint were measured, and a standard index finger model was established. Electromechanical characteristics of IPMC actuators were experimentally measured and mathematically modeled. These were incorporated into the dynamics of an index finger actuated by IPMC, and the dynamics of tip pinching were simulated. The arrangement of IPMC actuators at the initial position significantly affected the required actuator force to hold a given load. The maximum actuator force required to hold 0.98 N of fingertip load decreased by 50% for IPMC actuators that were arranged straight at the initial pinching position as compared to straight at the initial open position.

Manuscript received: July 25, 2012 / Accepted: August 13, 2012

1. Introduction

Active hand exoskeletons have been used to assist the activities of daily living (ADL) for physically weak people who are aged, injured, or handicapped. They are also used for rehabilitation purposes as well as power assist devices.[1] Most hand exoskeletons are actuated by electric motors[2-4] or pneumatic actuators,[5,6] and various power transmission methods such as cables,[2,7] gears,[4] linkages,[8] and pneumatics[5,6] are applied. Conventional electromechanical and pneumatic power systems have been used for power assistance and rehabilitation purposes, but their application to ADL assist devices has been limited, mainly due to their rigidity, high profile, and complex structures.

Electroactive polymers (EAPs) are good candidates for an exoskeleton actuator because their characteristics are similar to those of human muscles. They can generate force and deform in response to electrical stimulation[9-12] while they are flexible and lightweight. EAPs have been divided into electronic EAPs and ionic EAPs. Dielectric polymers, which are under the category of electronic EAPs, have been used as the actuators of orthotic and prosthetic devices,[13-15] but the high voltage requirement of electronic EAPs limits their applications. Among the ionic EAPs, ionic polymer metal composite (IPMC) has been tried in uses as artificial muscles for a biped walking robot[16] and heart assist device.[17] Low driving voltage and large strains are major advantages of IPMC actuators,[18] but small actuation force limits their applications as artificial muscles. Many efforts have been made to improve the electromechanical performance. An IPMC strip is quite attractive for a finger exoskeleton actuator because it is soft, light, and consumes little energy. Moreover, it does not require power transmission components, because the bending deformation of an IPMC strip conforms to finger flexion. It can also be used in an actuator integrated with a sensor.[19,20]

Dynamic analysis is important in developing hand exoskeletons and robot hands. Studies on the dynamics of finger exoskeletons have been performed in order to estimate work space, fingertip trajectories, and joint torque for index finger rehabilitation purposes.[8,21] Dynamic analysis has also been conducted to develop a control mechanism for a hand orthosis[22] as well as to predict the work space and force feedback mechanism for master-slave robot hands[23] and virtual reality simulations.[24] Most of the finger exoskeletons developed are actuated by electric motors, and the analysis is focused on the kinematics of

power transmission elements and the estimation of motor torque and rotation angles. The electromechanical characteristics of an IPMC actuator are unique; therefore, these should be properly modeled in order to analyze the dynamics of a finger exoskeleton actuated by an IPMC. However, a dynamic analysis incorporating proper modeling of an IPMC actuator has not been performed yet.

The dynamics of IPMC actuators has been analyzed for their possible applications as micro-manipulators,[25] swimming robots,[26] working robots,[27] and propulsion actuators,[28] but previous studies were limited to the modeling of the actuator itself. In designing a finger exoskeleton actuated by IPMCs, the dynamics of fingers actuated by an IPMC should be analyzed; therefore, proper modeling of the IPMC actuator and its application to finger dynamics should be performed. The prediction of fingertip pinching force generated by IPMC actuation is important in designing an exoskeleton, because of the limited capability of IPMC actuators to generate force, but this has not been studied yet. The goals of the present study are to develop an appropriate model of IPMC actuation and to apply this to analyze the dynamics of an index finger for a pinching task. The effects of actuator arrangement on the efficiency of fingertip force generation are also explored.

2. Methods

2.1 Biomechanical characteristics of an index finger

The finger exoskeleton is designed to fit over the index finger, and the IPMC actuator strip is located on the dorsal surface of the index finger. One end of an IPMC strip is fixed at the proximal site of a joint and the other end is positioned over the joint at the distal end of the phalange (Fig. 1). Bending of the IPMC strips by electric stimulation generates torque to rotate each joint. Three actuators are used to rotate the three joints of an index finger, which are the metacarpophalangeal (MCP), proximal interphalangeal (PIP), and distal interphalangeal (DIP) joints. We assume that the adductive and abductive movements of the MCP joint are restricted and that only the extension and flexion of each joint are allowed for a pinching task of an index finger. Anthropomorphic data on fingers were measured for 32 males aged 20 to 28 years. The length of each phalange of an index finger is measured as shown in Fig. 2.

An index finger model is represented by the three linkages with three joints, each of which has one degree of freedom (DOF). Lengths of linkages are determined on the basis of the measured anthropomorphic data on index fingers. Each joint is modeled by a linear spring and damper.[22,29] The stiffness constant of a joint is an important parameter in analyzing the dynamics of a finger; therefore, this is measured for the MCP joint. A load cell is located at the distal end of the proximal phalange, and the MCP joint is slowly rotated by pushing the load cell. The forces required to rotate the end of the phalange to the desired displacement are measured. Subsequently, the measured forces and displacements are converted to joint stiffness torques and rotation angles.

2.2 Characterization of the actuation performance of an IPMC strip

IPMC actuators are manufactured using Nafion membranes (N117, DuPont, USA). Five layers of Nafion membranes were placed between the presses (Model M, #9372, Fred S Carver, USA), heated up, and pressed with medium pressure as described in the previous study.[30] Platinum electrodes were created on both surfaces of the stacked membrane by a chemical reduction process, and IPMC actuators were finally fabricated. Transport of hydrated cations within an IPMC membrane under the applied voltage associated electrostatic interactions leads to mechanical deformation or bending of an IPMC membrane. Cation redistribution across the membrane by applied electric potential difference also generates water molecule redistribution which causes swelling near the cathode or mechanical strain. The IPMC membranes of 1 mm thickness were cut into strips with a width of 20 mm and used as the actuators of the finger exoskeletons. The lengths of actuators applied to rotate MCP, PIP, and DIP joints were 0.0426 m, 0.0240 m, and 0.0208 m, respectively.

An IPMC strip shows bending deformations when one end is cantilevered and an electric potential difference is applied between the electrodes that are plated onto both surfaces. The force generated by electrical stimulus at the free end of an actuator decreases as the tip deflection increases; therefore, maximum tip force is achieved when the deflection is zero. The reactive force that blocks further deformation of an IPMC strip under electrical stimulus is defined as the blocking force. Voltages with opposite polarities are applied to the separate electrodes on each side of an IPMC strip by a DC power supply (IT6720, Itech, South Korea), and the blocking forces are measured using a load cell (2002, NICOM, South Korea). Blocking forces at the tip of the IPMC actuator are measured for different tip deflections. Details of the experimental setup were given in the previous study.[31]

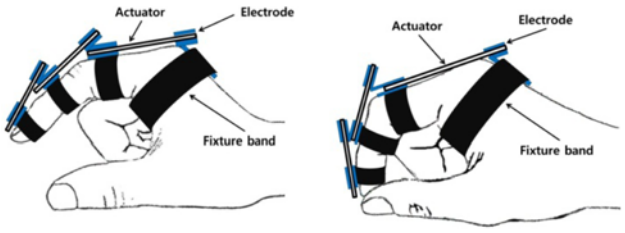

(a) Case 1 (b) Case 2

Fig. 1 Schematic diagrams of the finger exoskeleton. (a) Case 1: IPMC actuators are arranged straight in the initial open position. (b) Case 2: IPMC actuators are arranged straight in the initial pinching position

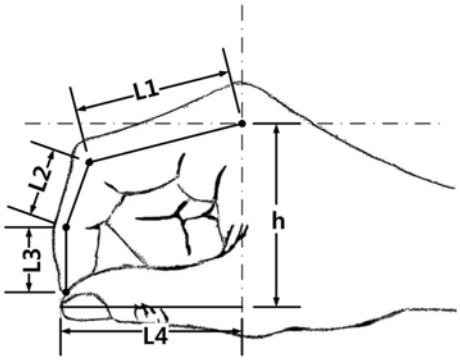

Fig. 2 Lengths between each joint and the tip of an index finger

2.3 Dynamic finger model

The pinch by an index finger tip is analyzed because that is the most representative and basic function performed in daily living. In this study, the pinching task is defined as the motion of an index finger to grasp a small object using the fingertip in the two-dimensional plane by rotating three joints. The thumb is assumed to be fixed, while abduction and adduction of the MCP joint are neglected; therefore, the dynamic behavior of an index finger is modeled as that of a three degree-of-freedom (DOF) serially linked planar manipulator as shown in Fig. 3. It is assumed that the pinching force is applied to the end of the distal phalange in the direction normal to the horizontal thumb. The reference frames for the angular motions of each joint are also shown in Fig. 3, and the counterclockwise directions of q_1, q_2, and q_3 represent the positive rotational senses of the MCP, PIP, and DIP joints, respectively.

When forces produced by IPMCs are applied to each phalange, the dynamic equations for each joint motion of an index finger can be expressed as follows:[32,33]

$$\begin{bmatrix} T_1 \\ T_2 \\ T_3 \end{bmatrix} = M(\Theta)\begin{bmatrix} \ddot{\theta}_1 \\ \ddot{\theta}_2 \\ \ddot{\theta}_3 \end{bmatrix} + B\begin{bmatrix} \dot{\theta}_1 \\ \dot{\theta}_2 \\ \dot{\theta}_3 \end{bmatrix} + K(\Theta) - J^T F_{pinch} + K(\Theta, \dot{\Theta}) + G(\Theta) \quad (1)$$

where T_1, T_2, T_3 denote the torques applied to each joint by IPMC actuators; M(θ) and B are the mass matrix and the damping coefficient matrix, respectively; K(θ), N(θ, $\dot{\theta}$) and G(θ) represent the torque vectors of the stiffness, Coriolis and centrifugal, and gravitational terms, respectively; F_{pinch} denotes the force vector applied to the fingertip due to the pinching task, and J^T is the transpose of the Jacobian matrix. Details on the mass matrix, the gravitational torque vector, the Coriolis and centrifugal torque vector, and the transposed Jacobian matrix that transforms pinching forces into joint torques are given elsewhere.[33]

The pinching force is modeled as the reactive force generated during the contact of the tips of an index finger and a thumb. Once the tips are in contact, the reactive force is increased from zero to the steady-state value by the forces generated by IPMC actuators. To model this contact process and reactive force generation, a spring and damper model is adopted between the tips. The reactive pinching force increases as the spring compression increases between the tips of the index finger and thumb, and the damping force is used to stabilize the contact model.

3. Results

3.1 Electromechanical characteristics of the IPMC

The blocking forces of an IPMC actuator were measured at the tip of an IPMC actuator as a function of time under the application of a 3 V direct current (DC) electric potential. The electric potential was limited below 3 V and experiments were performed in less than half an hour in order to minimize the effects of membrane water loss. The measured weight loss of the sample was within 5% of the total weight for each experiment. The blocking forces are normalized by the steady-state value, and they are shown in Fig. 4. Applying higher voltages would have increased the force, but the magnitude of the applied electric potential was kept below 3 V to minimize the loss of water by electrolysis in the IPMC. The generation of force by IPMC actuators is due to strain developed by the migrations of cations and water molecules near the cathode. The relationship between the input voltage and the charge in the IPMC can be modeled with a simple resistor-capacitor (RC) circuit because of the resistive and capacitive nature of electroactive polymers.[28] The force generation depends on the electric charge migration; therefore, the force generation of an IPMC under a step input voltage was considered using a simple first-order model. Back relaxation of the 1 mm thick IPMC actuators was negligible. The time constant (τ) of the first-order model was estimated from the force-time curve in Fig. 4, and this value was used to characterize the force generation of the IPMC actuators as a function of time:

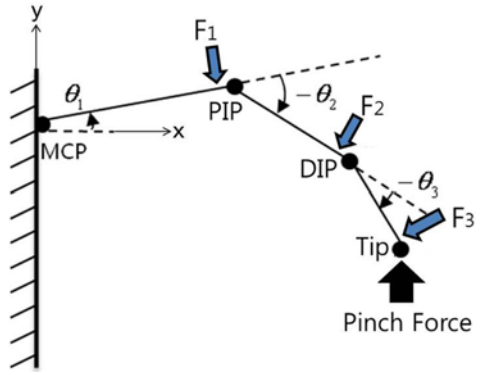

Fig. 3 Reference frames for the angular motion of each phalange of the index finger. Three IPMC actuators apply forces normal to the distal end of each phalange

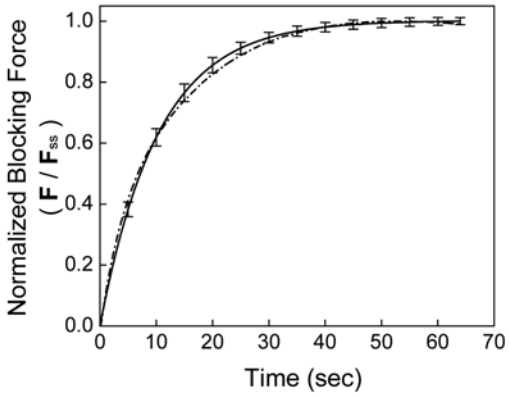

Fig. 4 The blocking forces normalized by the steady-state blocking force (F_{ss}) as a function of time. The solid curve shows the measured average force, and the dotted curve shows the first-order model $F(t)/F_{ss} = 1\text{-}e^{-t/\tau}$. Vertical bars show standard deviations

$$F(t) = F_{ss}(1 - e^{-t/\tau}) \quad (2)$$

where $F(t)$ is the blocking force, F_{ss} is the blocking force in the steady state, and t is time. The steady-state blocking force was 0.18 N and the time constant was 10.4 s for a 40 mm long actuator.

Blocking forces were measured at the free end of a cantilevered actuator for different vertical displacements caused by bending deflections. After the steady-state blocking force was measured at the tip of the IPMC in a straight position (no deflection), the load cell was moved to the location where the desired tip deflection was obtained using a micro-positioning stage. The steady-state blocking forces were

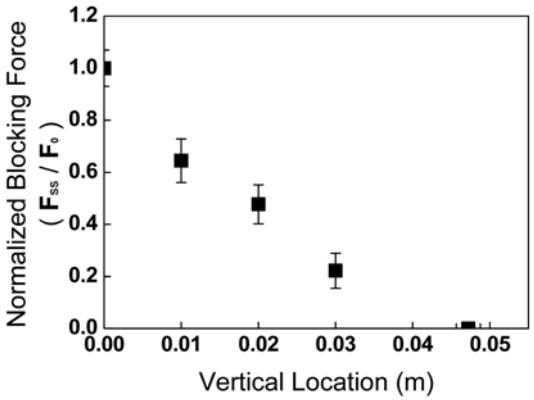

Fig. 5 The steady-state blocking forces (F_{ss}) normalized by the maximum blocking force without deflection (F_0) for different vertical locations. Vertical bars show standard deviations

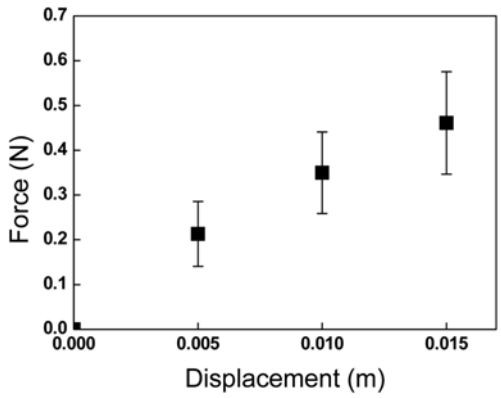

Fig. 6 Measured stiffness forces versus phalange tip displacement for the MCP joint. Vertical bars show standard deviations

Table 1 Index finger model parameters

See Fig. 1	Average Length (m)	Joint	Damping Coefficient (N · s/m)	Phalange	Mass (kg)
L1	0.0426				
L2	0.0240	MCP	0.0046	Proximal	0.0270
L3	0.0208	PIP	0.0027	Middle	0.0130
L4	0.0596	DIP	0.0020	Distal	0.0085
h	0.0496				

normalized by the maximum blocking force without deflection, and they are shown in Fig. 5. The blocking forces decreased as the deflection increased, and this relationship was modeled as the reduction in force generation due to the stiffness of an IPMC strip.[28] The actuation force of the IPMC, which was caused by ion movement, was partially used for bending the IPMC strip. Therefore, the available blocking force of an IPMC actuator was reduced for a deflected IPMC strip. The relationship between the steady-state blocking force F_{ss} and the vertical tip displacement (d) was approximated by a linear function,

$$F_{ss} = F_o(1 - k\delta) \tag{3}$$

where F_0 is the maximum blocking force without deflection and k is the slope of the force versus deflection curve.

3.2 Parameters of a dynamic finger model

Table 1 shows average values of the lengths between the joints of an index finger ($L1$, $L2$, $L3$), the length of a thumb ($L4$), and the length between the metacarpal phalangeal joints of an index finger and a thumb (h). The angles in the initial open position were assumed to be 4°, -25°, and -7° for the MCP, PIP, and DIP joints, respectively. The forces required to rotate the end of the proximal phalange to the desired displacement were measured in order to estimate the stiffness torque at the MCP joint. Fig. 6 shows the measured stiffness forces for different phalange tip displacements. Average stiffness forces and displacements are converted to a relationship between stiffness torque ($K(\theta)$) and rotation angle (θ) for MCP joints and then fitted to a third-order polynomial expressed as follows:

$$K(\theta) = (-3.3229\theta^3 - 0.3482\theta^2 + 1.6006\theta) \times l \tag{4}$$

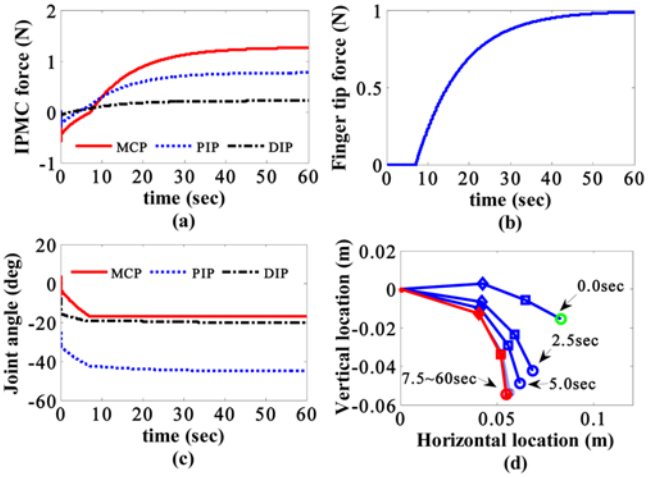

Fig. 7 Simulation results for pinching task (Case 1): (a) IPMC actuator tip force; (b) fingertip force; (c) joint angles; and (d) joint and fingertip locations

where l is the length of a phalange.

We assumed that PIP and DIP joints have the same stiffness torque-angle relationship as shown in equation (4). The mass of each phalange was obtained from the literature,[29] and the mass of the exoskeleton was neglected. The rotational damping coefficients, which do not seriously affect the dynamics of a pinching index finger, were determined using rectilinear damping coefficients obtained from the literature.[29] These parameters are listed in Table 1.

3.3 Actuation force at joints for different initial finger positions

The dynamics of pinching was simulated using the established models of the index finger and the electromechanical characteristics of IPMC actuators. The actuator forces required to hold a given tip load (0.98 N) were estimated. The pinching task was performed as follows: The index finger moved from the initial open position to the pinching position by a bending actuation of the IPMC strips. Once the pinching position was reached, the tip force increased to the required load (0.98 N). The blocking force generated by an IPMC actuator depended on the actuator deflection, and the maximum blocking force (F_0) that an IPMC actuator tip generated without deformation was defined as the force generating capability of the IPMC actuator.

Fig. 7 shows the simulation results for the pinching task when the

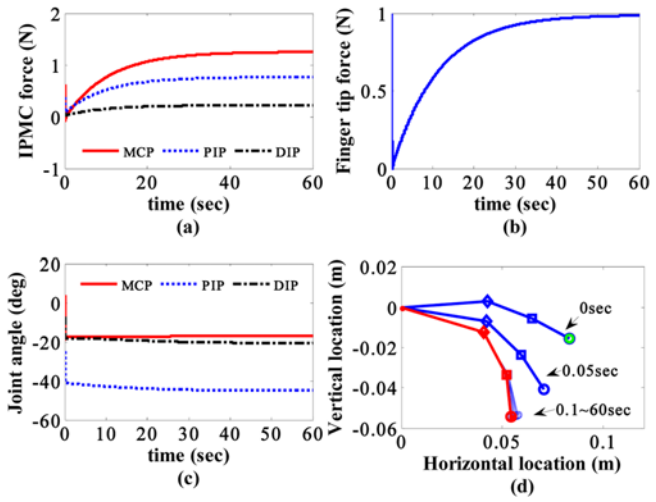

Fig. 8 Simulation results for pinching task (Case 2): (a) IPMC actuator tip force; (b) fingertip force; (c) joint angles; and (d) joint and fingertip locations

IPMC actuators are arranged straight in the initial open position (Case 1 in Fig. 1). In the open position, the distance between the tips of the thumb and index finger is about 4 cm, and the joint angles of the index finger are 4°, -25° and -7°, for the MCP, PIP, and DIP joints, respectively. Once the index finger reaches the pinching position, where the joint angles are -16°, -45°, and -22° for the MCP, PIP, and DIP joints, respectively, the reactive force at the tip increases to 0.98 N. Fig. 7 shows the IPMC actuator forces, the angle of each joint, the reactive force, and the joint locations. To hold 0.98 N at the pinching position, the forces required at the tips of the IPMC actuators are 1.26 N, 0.77 N, and 0.22 N for the MCP, PIP, and DIP joints, respectively. This result reveals that the IPMC actuator for an MCP joint should generate about 1.3 times more force than the tip load at the pinching position. Each actuator was straight at the initial open position but deformed at the pinching position. In order to estimate the force generating capability of an IPMC in the actuator arrangement of Case 1, the maximum blocking force (F_0) that an IPMC actuator tip generated without deformation was calculated. The values were 2.59 N, 1.50 N, and 0.32 N for the MCP, PIP, and DIP joints, respectively.

If we consider the negative slope of blocking force versus deflection for an IPMC actuator as shown in Fig. 5, the steady-state blocking force required of an IPMC actuator to hold the same tip load is reduced by decreasing the tip deflection at the pinching position. The IPMC actuator is arranged straight in the pinching position (Case 2 in Fig. 1), and the index finger is moved to the initial open position by applying the electric potential with the polarity opposite to that for the pinching actuation. The dynamics of an index finger pinching from the open position in Case 2 were simulated (Fig. 8). Each phalange rapidly moves to the pinching position, and the actuators generate forces to hold the 0.98 N fingertip pinching force. In order to hold the 0.98 N reactive force at the tip in the pinching position, the blocking forces that the IPMC actuators should generate in the steady state are 1.25 N, 0.76 N, and 0.22 N for the MCP, PIP, and DIP joints, respectively. These forces are close to the force generating capability of IPMC actuators or the maximum blocking force (F_0) because actuator deformations are negligible at the pinching position. If we compare the maximum blocking forces (F_0) for Case 1 with those for Case 2, the required maximum blocking forces for the actuators of the MCP, PIP, and DIP joints in Case 1 are about 2.0, 2.0, and 1.5 times greater than those in Case 2, respectively.

4. Discussion

IPMCs are good candidates for the actuators of a finger exoskeleton because of their muscle-like nature, but force generating capability would be their limiting factor for such an application. The dynamics of an index finger actuated by an IPMC from the open position to the pinching position were simulated for the case where IPMC actuators were arranged straight in the open position (Case 1), and the result showed that the IPMC actuator for the MCP joint should generate 1.26 N in order to hold the reactive force of 0.98 N at the index finger tip. Since bent IPMC actuators generate less force than undeformed ones, the initial actuator shape is an important design parameter. If the actuator is arranged straight in the initial open position, it deforms to reach the pinching position; therefore, the force generated at the actuator tip decreases due to bending deflection of the IPMC. In order to increase the blocking force at the pinching position, the IPMC actuators should be arranged straight in the pinching position (Case 2). Simulation results showed that steady-state blocking forces for the actuators at three joints in Case 2 were similar to those in the Case 1. However, the maximum blocking forces, which represent the force generating capability of the IPMC actuators, decreased by 50%, 49%, and 34% for the actuators of the MCP, PIP, and DIP joints in Case 2. Therefore, IPMC actuators with less force generating capability can be used to hold the same load if arranged straight in the pinching position.

If the IPMC actuator at the MCP joint is arranged straight in the pinching position, bending of IPMC in the dorsal direction is required to move the finger to the initial open position. Bending of the IPMC actuator in the direction opposite to pinching flexion can be achieved by switching the polarity of the applied voltage. A dynamic simulation of index finger extension driven by IPMC actuators from the pinching position to the open position was performed. The results showed that the maximum blocking forces required to extend the index finger to the open position were 1.35 N, 0.91 N, and 0.46 N. The largest of these maximum blocking forces required for extension is near the maximum blocking force of the MCP actuator in Case 2. Hence, flexion from the initial pinching position to the open position can be achieved with the actuators in Case 2.

The maximum blocking force measured for an IPMC actuator used in this study was less than the simulated maximum blocking force required for a pinching task. Efforts have been made to enhance the force generating characteristics.[34,35] One way to increase the blocking force is to stack IPMC strips layer by layer.[30] Our preliminary study indicates that stacking ten IPMC actuators and applying the electric potential of 3 V to each actuator generates a maximum blocking force of 1.8 N. Parallel arrangement of IPMC actuators by stacking can accumulate the force generated by each strip, but the increased thickness of the actuator may limit its applications.

5. Conclusion

In order to develop a finger exoskeleton with flexible polymer actuators, one was designed so that the three joints of an index finger were actuated by the bending of three IPMC strips. The mechanical characteristics of IPMC bending were experimentally measured, and these were incorporated into the dynamics of an index finger model. Due to the force and deflection characteristics of IPMC actuators, the arrangement of the IPMCs at the initial position affected the actuator force required for holding a given load at the pinching position. The maximum actuator force required to hold 0.98 N of fingertip load was decreased by 1.3 N, corresponding to a 50% reduction, for the case where the IPMC actuators were arranged straight in an initial pinching position as compared to an initial open position. Therefore, the force required of IPMC actuators to hold a given load can be reduced by an appropriate arrangement of the IPMC actuators.

ACKNOWLEDGEMENT

This work was supported by the Public Welfare & Safety research program through the National Research Foundation of Korea (NRF) funded by the Ministry of Education, Science and Technology [No. 2010-0020456].

REFERENCES

1. Gopura, R. A. R. C. and Kiguchi, K., "Mechanical designs of active upper-limb exoskeleton robots: State-of-the-art and design difficulties," Proceedings of the 2009 IEEE 11th International Conference on Rehabilitation Robotics, pp. 178-187, 2009.
2. Mulas, M., Folgheraiter, M., and Gini, G., "An EMG-controlled exoskeleton for hand rehabilitation," Proceedings of the 2005 IEEE 9th International Conference on Rehabilitation Robotics, pp. 371-374, 2005.
3. Sarakoglou, I., Tsagarakis, N., and Caldwell, D., "Occupational and physical therapy using a hand exoskeleton based exerciser," Proceedings of 2004 IEEE/RSJ International Conference on Intelligent Robots and Systems, pp. 2973-2978, 2004.
4. Wege, A. and Hommel, G., "Development and control of a hand exoskeleton for rehabilitation of hand injuries," Proceedings of the 2005 IEEE/RSJ International Conference on Intelligent Robots and Systems, pp. 3046-3051, 2005.
5. Lucas, L., DiCicco, M., and Matsuoka, Y., "An EMG-controlled hand exoskeleton for natural pinching," Journal of Robotics and Mechatronics, Vol. 16, No. 5, pp. 482-488, 2004.
6. Sasaki, D., Noritsugu, T., Takaiwa, M., and Yamamoto, H., "Wearable power assist device for hand grasping using pneumatic artificial rubber muscle," Proceedings of the 2004 IEEE International Workshop on Robot and Human Interactive Communication, pp. 655-660, 2004.
7. Mihelj, M., Nef, T., and Riener, R., "ARMin-toward a six DoF upper limb rehabilitation robot," Proceedings of the first IEEE/RAS-EMBS International Conference on Biomedical Robotics and Biomechatronics, pp. 1154-1159, 2006.
8. Cruz, E. and Kamper, D., "Use of a novel robotic interface to study finger motor control," Annals of Biomedical Engineering, Vol. 38, No. 2, pp. 259-268, 2010.
9. Bar-Cohen, Y., "Electroactive polymer (EAP) actuators as artificial muscles: reality, potential, and challenges, 2nd ed.," SPIE Press, 2004.
10. Shahinpoor, M. and Kim, K. J., "Ionic polymer-metal composites: III. Modeling and simulation as biomimetic sensors, actuators, transducers, and artificial muscles," Smart Materials and Structures, Vol. 13, No. 6, pp. 1362-1388, 2004.
11. Bar-Cohen, Y., "Electroactive Polymer Actuators and Devices (EAPAD)," Proceedings of SPIE's 6th Annual International Symposium on Smart Structures and Materials, 1999.
12. Mirfakhrai, T., Madden, J. D. W., and Baughman, R. H., "Polymer artificial muscles," Materials Today, Vol. 10, No. 4, pp. 30-38, 2007.
13. Herr, H. and Kornbluh, R., "New horizons for orthotic and prosthetic technology: artificial muscle for ambulation," Proceedings of the Smart Structures and Materials: Electroactive Polymer Actuators and Devices (EAPAD), pp. 1-9, 2004.
14. Pei, Q., Rosenthal, M. A., Pelrine, R., Stanford, S., and Kornbluh, R. D., "Multifunctional electroelastomer roll actuators and their application for biomimetic walking robots," Proceedings of the Smart Structures and Materials: Electroactive Polymer Actuators and Devices (EAPAD), pp. 281-290, 2003.
15. Ashley, S., "Artificial muscles," Scientific American, Vol. 289, pp. 52-59, 2003.
16. Yamakita, M., Kamamichi, N., Kaneda, Y., Asaka, K., and Luo, Z. W., "Development of an artificial muscle linear actuator using ionic polymer-metal composites," Advanced Robotics, Vol. 18, No. 4, pp. 383-399, 2004.
17. Shahinpoor, M., "Implantable Heart-Assist and Compression Devices Employing an Active Network of Electrically-Controllable Ionic Polymer-Metal Nanocomposites, in: Biomedical Applications of Electroactive Polymer Actuators," John Wiley, pp. 137-159, 2009.
18. Kim, C., Kim, S., Yang, H., Park, N., and Park, Y., "An Auto-focus Lens Actuator Using Ionic Polymer Metal Composites: Design, Fabrication and Control," Int. J. Precis. Eng. Manuf., Vol. 13, No. 10, pp. 1883-1887, 2012.
19. Yamakita, M., Sera, A., Kamamichi, N., Asaka, K., and Luo, Z. W., "Integrated design of IPMC actuator/sensor," Proceedings of the 2006 IEEE International Conference on Robotics and Automation, pp. 1834-1839, 2006.
20. Biddiss, E. and Chau, T., "Electroactive polymeric sensors in hand prostheses: Bending response of an ionic polymer metal composite," Medical Engineering and Physics, Vol. 28, No. 6, pp. 68-78, 2006.
21. Wang, J., Li, J., Zhang, Y., and Wang, S., "Design of an exoskeleton

for index finger rehabilitation," Proceedings of the 31st Annual International Conference of the IEEE EMBS, pp. 5957-5960, 2009.

22. Petroff, N., Reisinger, K. D., and Mason, P. A. C., "Fuzzy-control of a hand orthosis for restoring tip pinch, lateral pinch, and cylindrical prehensions to patients with elbow flexion intact," IEEE Transactions On Neural Systems and Rehabilitation Engineering, Vol. 9, No. 2, pp. 225-231, 2001.
23. Nakagawara, S., Kajimoto, H., Kawakami, N., Tachi, S., and Kawabuchi, I., "An encounter-type multi-fingered master hand using circuitous joints," Proceedings of the 2005 IEEE International Conference on Robotics and Automation, pp. 2667-2672, 2005.
24. Stergiopoulos, P., Fuchs, P., and Laurgeau, C., "Design of a 2-finger hand exoskeleton for VR grasping simulation," Eurohaptics, pp. 80-93, 2003.
25. Deole, U., Lumia, R., Shahinpoor, M., and Bermudez, M., "Design and test of IPMC artificial muscle microgripper," Journal of Micro-Nano Mechatron, Vol. 4, No. 3, pp. 95-102, 2008.
26. Nakabo, Y., Mukai, T., and Asaka, K., "Biomimetic soft robots using IPMC," Electroactive Polymers for Robotic Applications: Artificial Muscles and Sensor, pp. 165-198, 2007.
27. Yamakita, M., Kamamichi, N., Luo, Z., and Asaka, K., "Robotic application of IPMC actuators with redoping capability," Electroactive Polymers for Robotic Applications: Artificial Muscles and Sensor, pp. 199-225, 2007.
28. Yim, W. and Kim, K., "Dynamic Modeling of Segmented IPMC Actuator," Electroactive Polymers for Robotic Applications: Artificial Muscles and Sensor, pp. 263-277, 2007.
29. Arslan, Y. Z., Hacioglu, Y., and Yagiz, N., "Prosthetic hand finger control using fuzzy sliding modes," Journal of Intelligent Robotics Systems, Vol. 52, No. 1, pp. 121-138, 2008.
30. Lee, S. J., Han, M. J., Kim, S. J., Jho, J. Y., Lee, H. Y., and Kim, Y. H., "A new fabrication method for IPMC actuators and application to artificial fingers," Smart Materials Structures, Vol. 15, No. 5, pp. 1217-1224, 2006.
31. Lughmani, W. A., Jho, J. Y., Lee, J. Y., and Rhee, K., "Modeling of bending behavior of IPMC beams using concentrated ion boundary layer," Int. J. Precis. Eng. Manuf., Vol. 10, No. 5, pp. 131-139, 2009.
32. Park, K. C., "A Study on Position/Impact/Force Control of Redundant Robot Manipulators," M.S Dissertation, Mechanical Engineering, KAIST, 1993.
33. Craig, J. J., "Introduction to robotics, 2nd ed.," MA: Addison-Wesley Reading, pp. 195-210, 1989.
34. Lian, H., Qian, W., Estevez, L., Liu, H., Liu, Y., Jiang, T., Wang, K., Guo, W., and Giannelis, E. P., "Enhanced actuation in functionalized carbon nanotube-Nafion composites," Sensors and Actuators B: Chemical, Vol. 156, No. 1, pp. 187-193, 2011.
35. Jung, J.-H., Jeon, J.-H., Sridhar, V., and Oh, I.-K., "Electro-active graphene-Nafion actuators," Carbon, Vol. 49, No. 4, pp. 1279-1289, 2011.